ACS OMEGA

http://pubs.acs.org/journal/acsodf

Article

Study on Chemical Graft Structure Modification and Mechanical Properties of Photocured Polyimide

Zhiqiang Liu,[‖] Yilun Cai,[‖] Feifan Song, Jiajin Li, Jian Zhang, Yi Sun, Guoqiang Luo,* and Qiang Shen

Cite This: *ACS Omega* 2022, 7, 9582−9593

Read Online

ACCESS | Metrics & More | Article Recommendations | Supporting Information

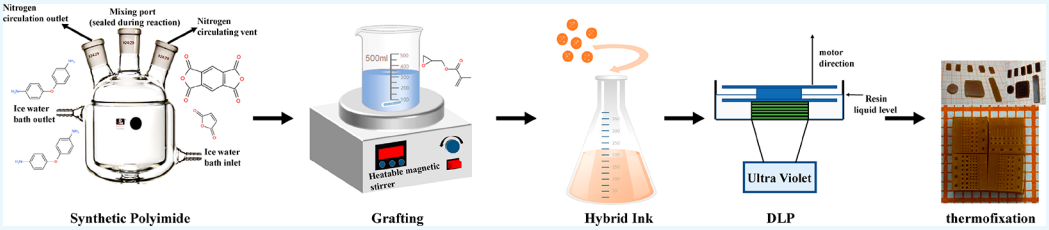

ABSTRACT: The great challenge facing additive manufacturing is that the available high-performance 3D printing materials can hardly keep up with the rapid development of new additive manufacturing technology. Then, the commercial resins available in the market have some problems, such as poor thermal stability, insufficient light-curing degree, and large shrinkage after curing, which need to be solved urgently. This study reports a photocurable polyimide ink for digital light processing (DLP) 3D printing to prepare controllable 3D structures with high thermal stability, low shrinkage, and excellent comprehensive properties. In this study, pyromellitic dianhydride and diaminodiphenyl ether, the Kapton polyimide with the highest performance synthesized so far, were selected as raw materials, and 2,2′-bis(3,4-dicarboxylic acid) hexafluoropropane dianhydride containing fluorine was introduced to modify the branched-chain structure. The polyimide was prepared by one-step imidization, and then the graft with photocurable double bonds and certain functions was grafted by reaction of glycidyl methacrylate with phenolic hydroxyl groups. In this work, the solubility of the synthesized oligomer polyimide in organic solvents was greatly increased by combining three methods, thereby allowing the formation of ink for photocuring 3D printing, and the ink can be stacked to form low-shrinkage polyimide with complex controllable shape. Polyimide printed by DLP can produce complex structures with good mechanical character and thermal stability and small shrinkage. Therefore, the polyimide prepared in this study is considered to be a resin of great commercial possibility. In addition, due to its properties, it has important development potential in some fields with high demand for thermal stability, such as high-temperature cooling valves, aerospace, and other fields.

1. INTRODUCTION

Additive manufacturing (AM), also known as 3D printing, is stacked in a bottom-up manner to form a complex three-dimensional structure. The preponderance of arbitrary shape control makes 3D printing widely used in various applications. Material jetting, material extrusion, vat photopolymerization, and powder bed fusion are the unique methods of AM, of which developments so far have emerged in stereolithography (SL), digital light processing (DLP),[1] two-photon lithography (TPP),[2] direct ink writing (DIW),[3] continuous liquid interface printing (CLIP),[4] fused wire manufacturing (FFF),[5] inkjet printing, and polymer powder layer fusion technologies.[6,7] These technologies can be seen in particular in some comments, which will not be described in detail here. As a method of additive manufacturing, photocuring has the advantages of being able to be molded at room temperature and having excellent geometric versatility on the strength of maintaining rapid prototyping in additive manufacturing,[7] which also makes it have a wide range of application potential in automotive, biomedical, aerospace, and other fields.[8] With the application demand of the designated field, it also puts forward higher requirements for the photocurable materials. At present, the photosensitive resin materials used in photocuring on the market generally have problems such as low strength, thermal stability, and properties that are difficult to merge, and the defect of low glass transition temperature (150 °C) also limits much application to a certain extent.[9]

Over the past few years, the research of photocurable materials has entered a bottleneck period, mainly because of the lack of high-performance materials combining mechanical properties, thermal stability, and chemical resistance. Many researchers are also developing novel materials for specific applications, such as chitosan hydrogels with growth and

Received: December 8, 2021
Accepted: February 25, 2022
Published: March 8, 2022

https://doi.org/10.1021/acsomega.1c06933
ACS Omega 2022, 7, 9582−9593

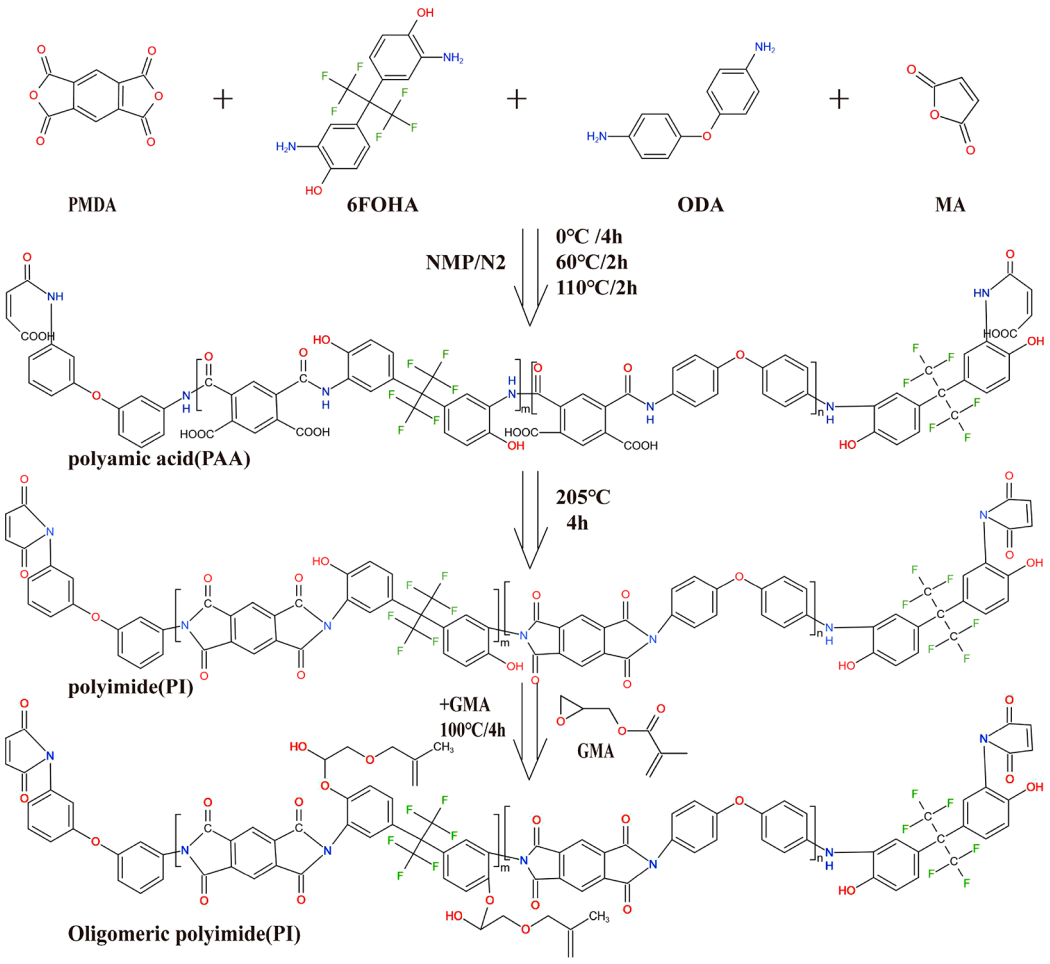

Figure 1. Reaction equation of preparation process of oligomer polyimide powder.

biocompatibility for biomedical applications,[10−13] high-performance isocyanates for space vehicles, and aerospace to automotive and electronics industries,[8] and functionally graded composite materials with hard and soft layers.[14] But the photocurable resins that these researchers have developed for the specific applications still do not combine many properties, into a single system. Recently, many researchers have focused their attention on a special functional material, polyimide, because it is one of the best organic polymer materials with comprehensive performance, and the research, development, and utilization of polyimide has led to it being listed as the most promising project in the 21st century.

Polyimide is a kind of polymer with an imide ring on the main chain. It has high- and low-temperature resistance, the long-term use temperature can be between −200 and 300 °C, and it has excellent mechanical properties (tensile strength ⩾ 100 MPa; bending strength ⩾ 170 MPa) and chemical and corrosion resistance, so it has a wide range of applications in aerospace, automotive, and other fields.[15−19] Gouzman et al.[19] mainly describe the modification of polyimide (PI) and introduce the three-dimensional polyimide structure made by additive manufacturing or thermoforming, which can expand the space application of polyimide and has a guiding reference for the research of polyimide. However, the rigid main chain structure of polyimide makes it have poor solubility and a high melting point, so it has obvious defects such as difficult molding, difficult shape control, and high molding cost. The advantages of fast curing, room-temperature operation, high-quality final products, and low cost can overcome the above defects. Therefore, the combination of these two research fields has become the most concerned issue of current researchers. The photocurable resins used in DLP and SLA are generally composed of unsaturated monomers/oligomers that can be excited by ultraviolet light sources, diluents that reduce viscosity and increase fluidity to ensure printing, and photoinitiators. Polyimide itself does not have unsaturated bonds and has difficulty being soluble in various organic solvents, so it is difficult to adapt to the photocuring molding method. Many scholars have also tried various methods to add polyimide into the laminated additive manufacturing system. Hegde et al.[20] attempted to produce the prepolymer PMDA−ODA polyamic acid (PMDA, pyromellitic dianhydride; ODA, 4,4′-diphenyl either diamine) through intermolecular cis−trans cross-linking. After printing and molding, a two-step heat treatment was performed to obtain a photocurable sample with a controllable shape that was closest to the molded form of polyimide. The team has also produced the best performing polyimide ever manufactured by additive manufacturing molding. Inspired by Hedge et al.'s work, Herzberger's research group formed polyamides by introducing the carboxyl group of 2-(dimethylamino)ethyl methacrylate (DMAEMA) and polyamides based on the former process and formed the UV-sensitive group that can be cured by light.[21] After that, removal of DMAEMA during the postcuring process also provided the high-performance polyamides. In addition, the team also improved the printing method by combining DIW

https://doi.org/10.1021/acsomega.1c06933
ACS Omega 2022, 7, 9582−9593

Table 1. Proportion and Function of Each Component in Oligomer Synthesis

monomer	NMP	PMDA	ODA	6FOHA	MA	GMA
content (%)	67	15	8	5	2	3
function	solvent	provides aromatic structure	provides aromatic structure	provides trifluoromethyl	end-capping agent	change the structure of oligomer branch chain

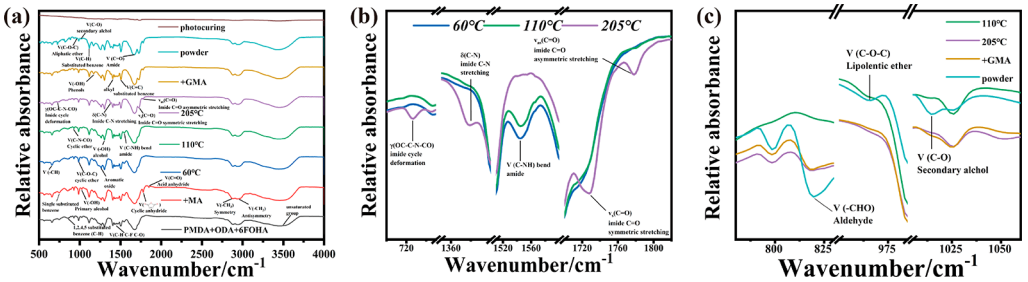

Figure 2. (a) Infrared comparison of the whole reaction process. (b) Amide characteristic peak, 1544 cm^{-1} (CNH); imide characteristic peaks, 727 cm^{-1} (OC−C−N−CO), 1378 cm^{-1} (C−N), and 1727 cm^{-1} (C═O). (c) Secondary alcohol characteristic peak, 1015 cm^{-1}; characteristic peak of aliphatic ether, 966 cm^{-1}.

and UV curing to improve the printing resolution.[22] Although they all obtained high-performance photocurable polyimide resins, these resins all had some problems, such as a large shrinkage rate (45−55%) when removing solvent during the postcuring period. Mohamed and Kuo, Rusu et al., and Shi et al.[23−25] discuss various methods of inserting nanoparticles into a PI matrix by covalent chemical bonding and physical blending, which have enlightening suggestions for the modification of polyimide. Guo et al.[26,27] and Li et al.[28] are also aware of the problem wherein the shrinkage rate of post-treatment affects dimensional stability. They are committed to solving the solubility of polyimide by introducing the main chain of polyimide as a side chain through chemical modification grafting technology so that the polyimide is more suitable for photocuring molding. This chemical grafting technique improves the solubility of polyimide in organic solvents, resulting in a higher solid content of oligomer precursors, and, to some extent, reduces the shrinkage of subsequent curing. But it also damages its mechanical properties. Some scholars[29−31] have also tried new ideas, considering the combination of traditional manufacturing methods and additive manufacturing methods or the combination of several different printing methods to produce the required 3D objects.

Existing studies show that the main problems of light-cured polyimides lie in the following three aspects. First, there is the adaptability of polyimides to photocuring. Second, mechanical strength, printing resolution, and shrinkage cannot happen simultaneously. Finally, there are few studies on postcuring.

Here, for the first, high-temperature imide in the synthesis process is proposed to solve the shrinkage problem from the root. Kapton-type polyimides PMDA and ODA are used as dianhydride and diamine monomers to maintain the characteristics of high-performance polyimide, and fluorine-containing diamine is introduced to increase the solubility of the products in organic solvents to some extent so that the subsequent polyimide resin has better fluidity and is more suitable for photocuring molding. In addition, the mechanical properties and thermal stability of the photocurable polyimide resin were studied. The influence of different parameters of molding and postcuring on its properties was investigated. The influence of postcuring on shrinkage in different directions was investigated systematically, which provides some reference for the strict design of dimensional stability. The printed polyimide samples have high mechanical properties and thermal stability, and their excellent dimensional stability makes them have great potential applications in aerospace, automotive, and other fields with high thermal stability requirements.

2. RESULTS AND DISCUSSION

2.1. Synthesis and Characterization of Grafted Polyimide Oligomer. Recently, we used the advanced iridized method to synthesize polyimide which can be used in photocurable shrinkage manufacturing, providing new ideas for solving polyimide solid shrinkage problems. Specifically, to the monomer PMDA, ODA, which is the highest synthesis of Kapton-type polyimide, is added to ensure its strength and thermal stability. Then, the fluorine-containing diamine is added to increase the solubility of the product in the organic solvent. PMDA, ODA, and fluorinated diamine were added to the organic solvent *N*-methylpyrrolidone (NMP) at 0 °C and stirred at constant temperature for 4 h. Amino reacts with an anhydride to form polyamide acid (PAA) and then gradually increases the temperature by dehydration cyclization and imidization to form oligomer PI, which is cooled and grafted into glycidyl methacrylate (GMA) reaction; the specific reaction process is shown in Figure 1. In addition, we also summarize the mass fraction of each component of the synthesized oligomer and its function in Table 1. PMDA and ODA are Kapton polyimide monomers, which provide benzene ring structure, and 6FOHA provides trifluoromethyl, which can increase optical transparency and make them suitable for photocuring. GMA, as a grafting structure, on the one hand, introduces unsaturated double-bond structure; on the other hand, the branched structure improves its solubility and has a significant effect on the improvement of interlayer bonding force.

The chemical structure of the synthesized polyimide oligomer was determined by FT-IR. The results show that the chemical structure of the synthesized polyimide oligomer is shown in Figure 11. We assign all of the spectral peaks of FT-IR characterization results, and the calibration results are shown in Figure 2a. Under the reaction conditions of 60 and 110 °C, the disappearance of the characteristic peak of cyclic

https://doi.org/10.1021/acsomega.1c06933
ACS Omega 2022, 7, 9582−9593

Table 2. Proportion and Function of Each Component in Ink Formation

component	PIs	NVP	TMPTA	PEG400	LMA	TPO
content (%)	30	27	25	10	5	3
function	oligomer	solvent	improve toughness	improve toughness	improve the bond strength between layers	photoinitiator

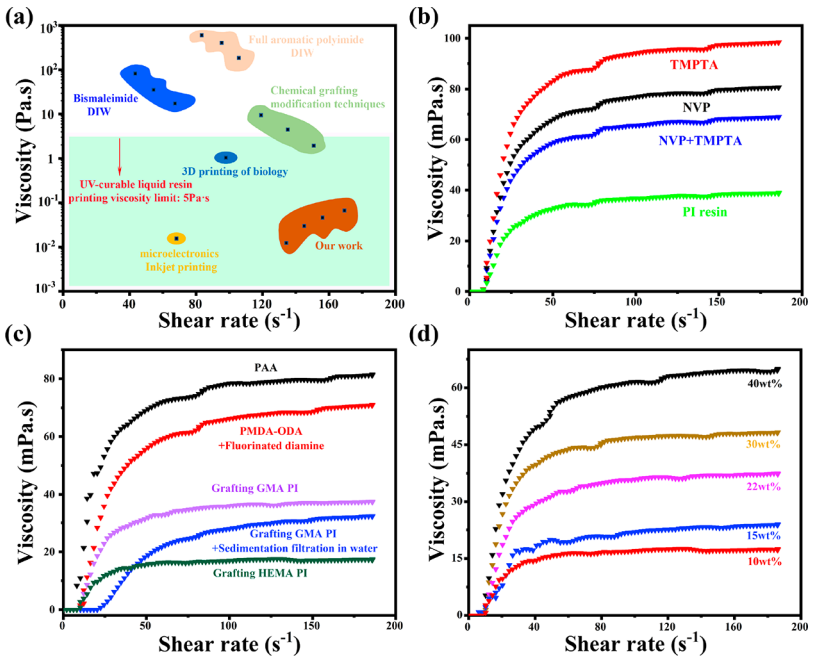

Figure 3. (a) Range of printing viscosity achieved by changing various printing methods and combining solutions in the literature. (b) Comparison of viscosity of different diluents and shear viscosity of the prepared resin. (c) Several different attempted ways to synthesize oligomers from monomers and comparison of the shear viscosity of different processes. (d) Comparison of shear viscosity of different oligomer polyimide content.

anhydride at 1750−1800 cm^{-1} indicates the completion of dianhydride reaction, while the characteristic peak of amide (C−-NH) at 1544 cm^{-1} indicates the formation of polyamide. In addition, comparing the infrared spectra at 205 °C with those at 60 and 110 °C, the characteristic amide peak (C−NH) of the former disappeared at 1544 cm^{-1} and the characteristic imide peaks appeared at 727 cm^{-1} (OC−C−N−CO), 1378 cm^{-1} (C−N), and 1727 cm^{-1} (C═O), which all indicate that imidization is complete at 205 °C (as shown in Figure 2b).

FT-IR results of the powder obtained by precipitation filtration showed that the appearance of the characteristic peak of secondary alcohol at 1015 cm^{-1} represented the opening of GMA aliphatic cyclic ethers, and the first appearance of aliphatic ethers at 966 cm^{-1} (Figure 2c) revealed the successful grafting of GMA. In addition, we performed solid state NMR hydrogen spectra of oligomers, printed samples, and postcured samples, and the results are shown in Supporting Information Figure S1.

2.2. Preparation of PI-Based Resin. Generally, photocurable ink[6,32−34] consists of prepolymer, reactive diluent, and photoinitiator, and some additives are added for functional structure. Prepolymer generally has one or more functional groups, which will affect the curing speed, cross-linking density, and the performance of the final part. The reactive diluent is added to reduce the viscosity of the prepolymer and facilitate molding. Microscopically, the curing process is mainly divided into three stages. First, ultraviolet radiation is transmitted through the photoinitiator, causing the excited rearrangement and generating free radicals. Then, the excited rearrangement free radicals react with unsaturated bonds in prepolymer molecules, causing the chain growth in the prepolymer. Finally, after the free radicals lose their activity, the low molecules of the reaction system cross-link and solidify into three-dimensional reticular macromolecules, which shows that the liquid state is transformed into solid state macroscopically. Here we provide the mass fraction and function of each component of the resin prepared in this work (see Table 2). The introduction of LMA[35] can improve the interlayer bonding performance of printed samples, and 3% photoinitiator[36] content can provide the maximum photoinitiation efficiency.

2.3. Fluidity and Adaptability to Light Curing. The polyimide has a rigid backbone structure to cause it to have poor solubility, and it is difficult to solute in many organic solvents so that it is difficult to adapt to a printing method manufactured by the addition. Our group innovation uses three ways to modify its solubility in an organic solvent. First, the fluorine diamine is modified in monomeric structures. Atomic fluorine or trifluoromethyl is greatly improved to polyimide, and the optical transparency is improved,[37,38] which is essential for polyimide adapted to additive manufacturing.[39] In addition, the team modified polyimide solubility by chemical grafting techniques. GMA can be grafted into the polymer due to the presence of a highly active acrylate double bond, and the epoxy groups contained in GMA can be reacted with a variety of other functional groups to form a functionalized polymer. The team grafted GMA on the polyimide branches, not only modifying polyimide solubility but also achieving a toughening effect.[40] At the same time, the introduction of GMA with an aliphatic side group enhances the

https://doi.org/10.1021/acsomega.1c06933
ACS Omega 2022, 7, 9582−9593

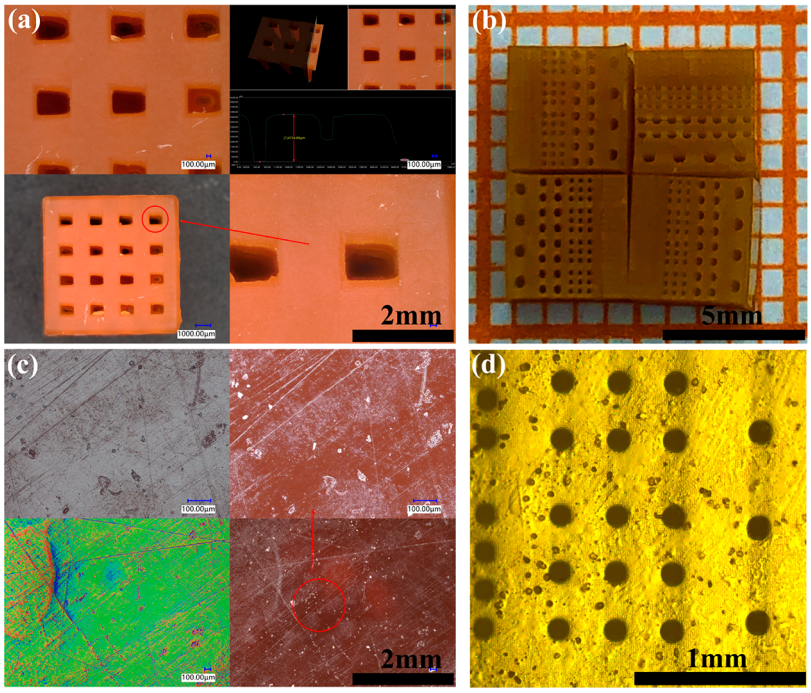

Figure 4. (a) Ultra-depth-of-field microscope image capturing the print sample of the photocuring printer (sample design size, 10 × 10 × 10 mm^3; aperture 1000 × 500 μm^2). (b) Gradient porosity print sample map (design size, 4 × 4 × 4 mm^3; minimum aperture, 100 μm). (c) Macroscopic surface of the sample showing that the slight scratch on the surface of the sample is the result of etching after ethanol treatment. (d) Photograph of the sample shown in panel b by optical microscope showing that the surface molding is complete without damage.

transparency of polyimide, which is necessary for UV light curing to increase the light depth. Last, but not the least, our group used precipitation filtration in water to redissolve in the diluent rather than directly dissolve in the diluent. Our belief is that this step can improve the solubility of polyimide by destroying the symmetry and regularity of the main chain of polyimide molecules and increasing the free volume content in the material. The soluble powder dissolves in the diluent to obtain the less viscous resin, and the excellent fluidity makes it a perfect combination with additive manufacturing. The fluidity of the resulting resin is shown in Figure 3b,c. Our group combined three ways to improve the solubility so that the resin fluidity reached the level of centipoises, which was a great improvement compared with the level of pascal-second obtained by other groups (Figure 3a), which also provided the possibility for the resin prepared by our group to realize DLP additive manufacturing of high resolution.

In addition, we studied the relationship between viscosity and different solid content (mass ratio of polyimide to organic solvent). The results show that (as shown in Figure 3d), with the increase of solid content, its viscosity also increases correspondingly, and this high solid content also benefits from its high solubility in organic solvents. Interestingly, we found that the resins prepared in this work exhibit shear thickening. We analyze this because the preparation of the resin is a multiphase mixture system, containing acrylate and other solid content systems;[41] in addition to this, we are investigating polyimide solubility modification but have still failed to achieve the high polyimide solid content type resin: polyimide solid content is relatively low so wettability is bad.[42] When the external force is applied, the original dense structure is destroyed and a new structure is formed. It is worth mentioning that we found that the viscosity of the prepared resin would decrease with the increase of temperature. We believe that the increase of the distance between the liquid molecules makes the intermolecular attraction decrease, so the internal friction decreases, resulting in the decrease of the viscosity of the liquid. In addition, with the increase of storage time, its viscosity increased significantly, but it was still in a small printing viscosity range.

2.4. Characterization. A DLP 3D printer is used to produce 3D architecture by stacking photocured polyimide layer by layer. First, the 3D model of the set architecture entity is drawn by computer software, then imported into DLP printer by computer in STL format, and converted into a series of single-layer 3D images in the form of digital slices. Finally, the polyimide resin in the curing chute is controlled to solidify and stack layer by layer by ultraviolet projection, until the whole design 3D object is formed. The macrosurface of the printed polyimide sample is shown in Figure 4a,b. Under the ultra-depth-of-field microscope, hundreds of micrometer-sized voids can be completely penetrated and clearly seen, which is due to the high resolution of the stereolithography apparatus method. Panels c and d of Figure 4 show the macroscopic picture under the ultra-depth-of-field microscope and the aperture picture under the optical microscope after being cleaned by ethanol. The controllable aperture can reach 100 μm, which provides unlimited development potential for photocuring high-precision printing.

Our group observed the microscopic morphology of the printed sample section, and we could observe the obvious layer structure (as shown in Figure 6a). However, after we have improved the print parameters and the printing ink is dispersed, the combination between the layers is denser and the section SEM map is shown in Figure 5b. After the postcured heat treatment (220 °C/4 h), the layer bond is closely observed and the layer structure is not observed (Figure

https://doi.org/10.1021/acsomega.1c06933
ACS Omega 2022, 7, 9582−9593

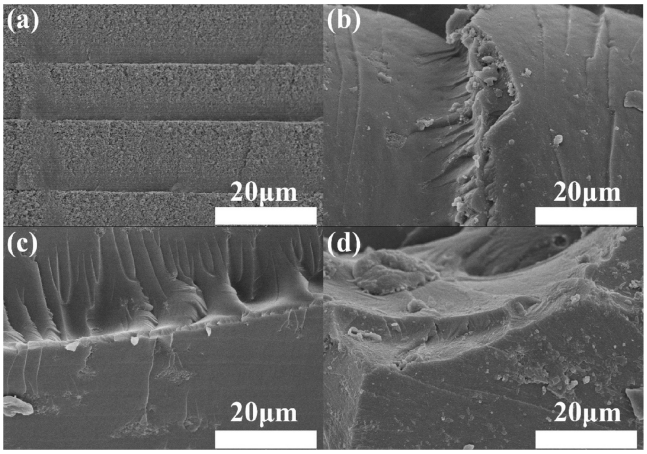

Figure 5. (a) Sample section scanning electron microscope (printed single-layer thickness, 20 μm). (b) Scanning electron microscope image of the sample section showing that the printed sample layer thickness is 20 μm and the curing time is 11 s. (c) Scanning electron microscope image of the sample section showing that the printed sample layer thickness is 20 μm and the curing time is 13 s. (d) Scanning electron microscope image of the sample section showing that the printed sample layer thickness is 20 μm and the curing time is 15 s.

5c,d). This is because of iridization and presentation as a macroscopic surface to be complete!

2.5. Mechanical Properties. The resin printed by light curing has the problems of low strength and poor mechanical properties after printing. In our work, Kapton polyimide PMDA−ODA is used as dianhydride and partial diamine as the monomer; the former is the monomer with the highest mechanical properties of polyimide so far, so the mechanical properties of our resin printed by light-curing (DLP) are better than those of ordinary commercial resin to some extent, but it still does not reach a satisfactory height. In this work, the degree of curing is increased by further postcuring, which is expected to bring significant effect for the improvement of mechanical properties.[43,44] Shear and compression expression experiments show that the mechanical properties of DLP printed by light curing are improved after heat treatment at 190 °C for 3 h. There are two reasons for this analysis. First, due to the low cross-linking degree, some active diluent NVP polymerization[45] occurs in an environment close to the melting point. In the process of photocuring, free radical initiator also converts NVP into poly(vinylpyrrolidone), and the increase of molecular weight improves its mechanical properties. The microscopic performance is that its links are more closely connected, so it needs higher energy to break and its mechanical properties are higher. On the other hand, due to the ultraviolet light energy and the photosensitivity of the prepared resin, the polyimide is incompletely cured after digital light process printing, and the curing degree is further improved at 190 °C, so its mechanical properties are also higher. Moreover, we believe that glycidyl methacrylate will also affect its mechanical properties. As GMA grafted with unsaturated double bonds, there may be insufficient polymerization after UV curing, so there may be incomplete polymerization of unsaturated double bonds. However, during thermal curing, part of the unsaturated double bonds are further polymerized with the temperature rising, the degree of polymerization is further improved, and its molecular weight is higher, so its mechanical properties are better.

In addition, the parameters of UV-curing printing of synthetic resin were also studied. The curing depth of light curing is mainly related to the photosensitivity of resin. At present, most researchers use the Jacobs equation to describe the curing depth:[3,6,11,14,46]

$$C_d = D_P \ln(E_0/E_c)$$

In which C_d is the curing depth, E_0 is the energy density of incident ultraviolet light, E_c is the critical energy density to be cured, and D_p is the sensitivity of photocuring, that is, the depth of light transmission. The prepared resin can be cured to form the required 3D component only after the ultraviolet energy exceeds the critical energy density to be cured. Given this, we explored the influence of different parameters, including single-layer thickness and single-layer curing time on the curing effect. Combined with SEM micrographs, it is the observer that if the thickness of the single layer is designed to be 20 μm, the curing is incomplete, forming a natural gradient distribution and fine pores; When the thickness of the single layer is designed to be 10 μm, no layered structure can be observed in the microstructure and the bonding is very dense, which is consistent with the calculation of the Jacobian equation. Our team provided the experimental steps and schematic diagrams of stretching, shearing, and compression. First, we printed the sample structure designed by computer (tensile sample: sample size is shown in the Support Information Figure S2) by DLP (error, ±0.1 mm). Subsequently, samples before and after the thermal curing (as shown in Figure 11) are put through, as shown in Figure 6, shear, tensile, and compression experiment devices for testing. The results are shown in Figure 7 and Figure 8. It can be seen that the mechanical properties decrease greatly with the increase of monolayer thickness, and the shear strength of the sample with monolayer thickness of 10 μm is up to 28.2 MPa. Moreover, our team also discussed the curing time of a single layer for samples with the same thickness as a single layer. As shown in Figure 6c, the curing time of the single layer is set to 11−15 s. It is obvious from the figure that the mechanical properties of the single layer are significantly enhanced with

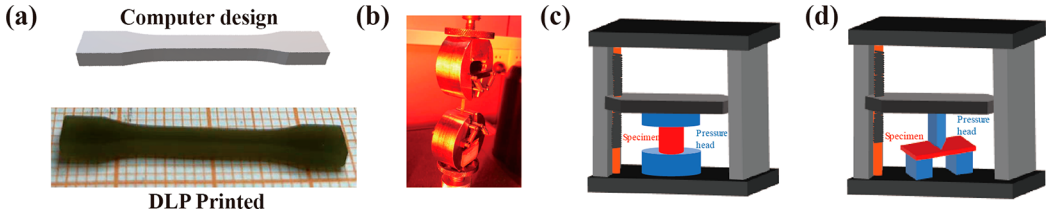

Figure 6. (a) Comparison between computer designed sample size and actual DLP printing (error, ±0.1 mm). (b) Tensile specimen stretched by universal mechanical testing machine. (c) Schematic diagram of compression experiment. (d) Schematic diagram of shearing experiment.

https://doi.org/10.1021/acsomega.1c06933
ACS Omega 2022, 7, 9582−9593

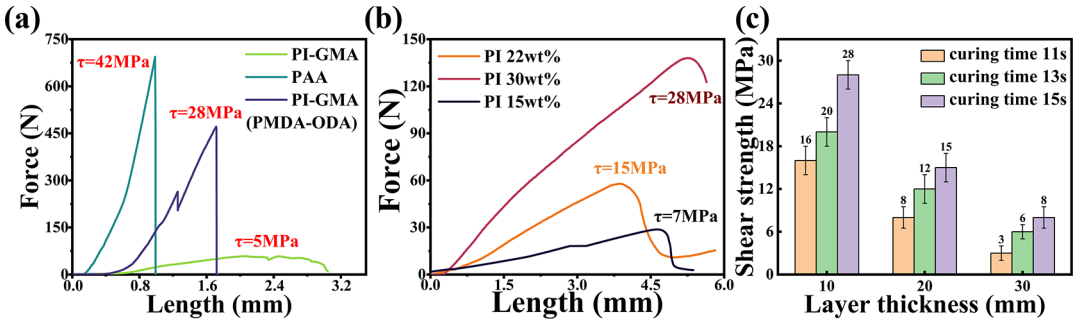

Figure 7. (a) Shear strength under different monomer and graft chemical structures. (b) Shear curves of samples obtained by photocuring printing resins with different mass fractions. (c) Influence of printing parameters on its mechanical properties (layer thickness, 10−30 μm; curing time, 11−15 s).

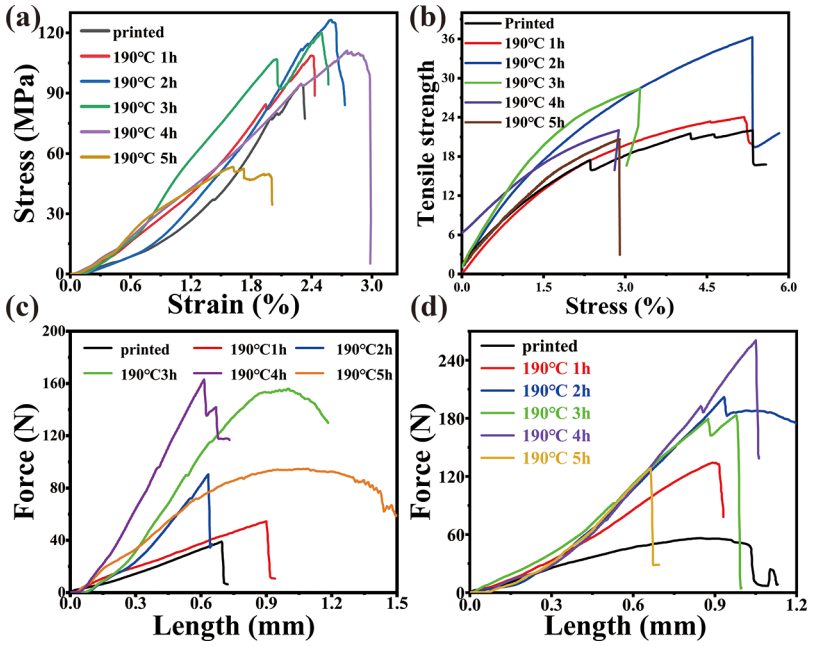

Figure 8. Effect of postcuring on mechanical properties: (a) Curing at 190 °C for 1−5 h to test its compressive stress−strain curve; (b) curing at 90 °C for 1−5 h to test its tensile strength; (c) printing of the shear curve of the sample in the layer stacking direction; (d) printing of the shear curve of the sample in the direction perpendicular to the layer stacking.

the increase of the curing time of the single layer. Figure 5 SEM diagram mentioned above shows good surface properties and excellent interlayer bonding properties.

Interestingly, when exploring the mechanical properties of single-layer curing time and thickness,[47−49] we found an interesting experimental phenomenon—the mechanical properties of printed samples are closely related to the printing direction. Because of this, we have entered into an in-depth study of this phenomenon. Our group has carried out thermal curing on the samples in a 190 °C air drying oven while keeping the curing time and thickness of the single layer the same and explored the changes in their mechanical properties. Several groups of samples were cured by heat treatment for a different time, and shear, compression and tensile experiments were carried out. The shear and tensile tests (such as in Figure 8b,c) show that the mechanical properties increase significantly with the increase of heat treatment time at 190 °C, but decrease after more than 3 h. Our analysis indicates that this is because the mechanical properties of the polymer bonds are destroyed after the complete polymerization is completed after more than 3 h. In the tensile test, with the extension of heat treatment time, the stress increases significantly, but the strain decreases gradually, which shows that the strength of the sample is enhanced and the toughness is relatively decreased by heat treatment. When we compare the shear strength in the stacking direction and the vertical and stacking direction in the shear experiment, we find an interesting phenomenon. It was observed that the shear strength and compression modulus in the vertical and printing directions were significantly higher than those in the parallel printing direction. Our analysis determined that this is due to the characteristics of addition of the improvement materials, and the characteristic of the rapid molding of the addition of the reducing material makes it better before the layer is lower than the layer, and thus the mechanical properties are lower. Given this, our team increased its solidification again by heat curing. The results show that after thermal curing, the mechanical properties parallel to the print direction are varied to the mechanical properties in the vertical and printing direction (as shown in Figure 9), which is because the degree of cure deepened the combination, which is also consistent with the previous analysis. In addition, the difference of shear strength between

https://doi.org/10.1021/acsomega.1c06933
ACS Omega 2022, 7, 9582−9593

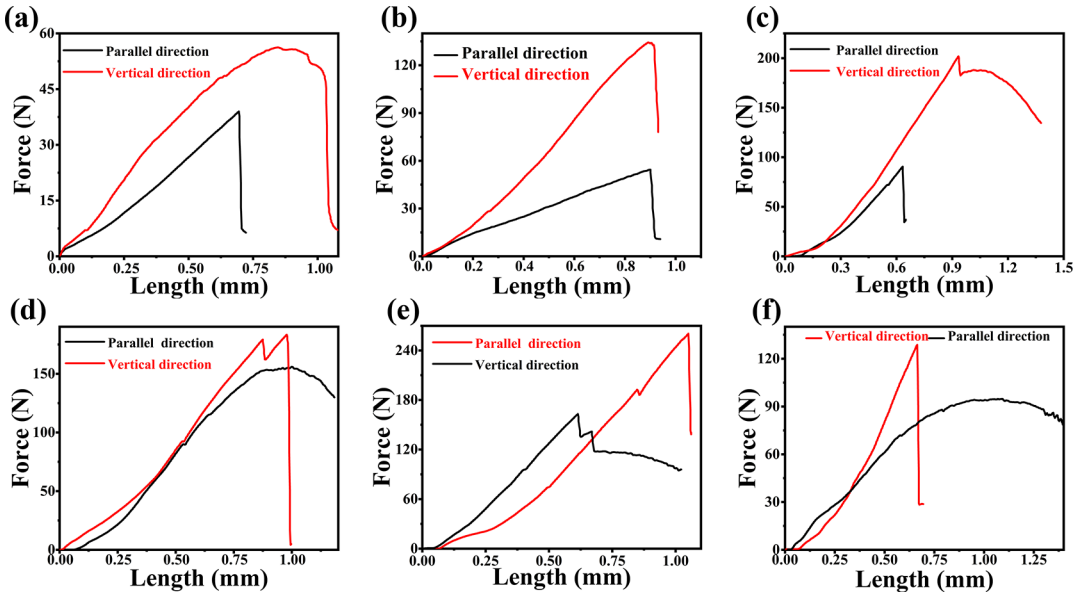

Figure 9. Comparison of mechanical properties perpendicular to the layer stacking direction and parallel to the layer stacking direction: (a) no thermal curing occurred; (b) 190 °C, 1 h; (c) 190 °C, 2 h; (d) 190 °C, 3 h; (e) 190 °C, 4 h; (f) 190 °C, 5 h.

vertical direction and parallel direction reaches the minimum, which indicates that the optimal heat treatment condition is 190 °C for 3 h.

2.6. Thermal Stability. Polyimide is one of the highest performance organic polymer materials, and its unique advantage is that its long-term use temperature can be used for −200 to 300 °C. At present, commercially available photocurable resins cannot achieve high-temperature use requirements, and thermally decomposing temperatures are below 200 °C, while the photocurable polyimide oligomer powder prepared by this work is thermally decomposed below 300 °C (as shown in Figure 9), this is also closely related to the synthetic monomers we used. For polyimide synthesized from *p*-xylenedic acid dianhydride and phenylenediamine, the thermal decomposition temperature can be as high as one of the most thermally stabilized varieties in the polymer, and Kapton PMDA with ODA as monomer was also used in this work. The dianhydride and phenylenediamine introduce fluorine-containing diamine, and chemically modified grafting techniques are modified, the chain structure is increased, the solubility is increased, and the thermal stability is damaged. Its thermal decomposition temperature is much lower than 600 °C. But although only 300 °C, it is better than currently photocurable commercial resins, providing greater development potential for high-temperature application of resins. In order to explore the preparation of powder and thermal stability of resin, several experiments were carried out. Thermogravimetric analysis (TGA test condition: nitrogen; room temperature to 1000 °C; heating rate, 10 °C/min) was performed on Kapton polyimide powder synthesized in this work and resin prepared by different monomers. The results are shown in Figure 9. The result shows that the thermal decomposition temperatures[50−54] of linear PI and fully aromatic PI are significantly different. Compared with linear PI, the thermal decomposition temperature of all-aromatic polyimide is linear PI, mainly because all-aromatic PI has more benzene rings and a stable structure, which requires a higher temperature to break its bond energy. However, the linear polyimide chain structure is unstable and easily damaged, so the thermal decomposition temperature is low. However, the thermal decomposition temperature of aromatic polyimide grafted GMA powder synthesized in this work is somewhat different from that of fully aromatic powder, but it is still better than that of linear polyimide. This is also because the branched structure is introduced with grafting, but the existence of the benzene ring structure of the Kapton monomer is still difficult to destroy. For the TGA results, we assigned the mass losses at different temperatures and compared the boiling point; these mass losses were consistent with the content we added. As shown in Figure 10, the yellow curve is the TGA of the sample

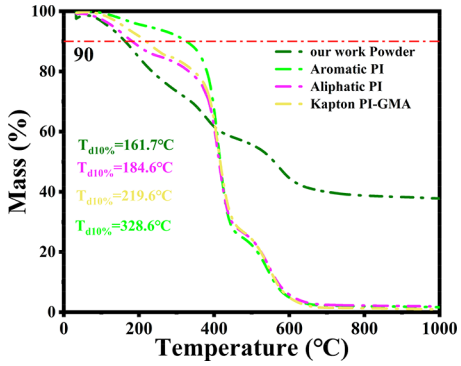

Figure 10. TGA test curves of powder and printed samples (test conditions: nitrogen; room temperature to 1000 °C; heating rate, 10 °C/min.).

after DLP printing in the powder dissolved in NVP and TMPTA. Combining the boiling points of NVP and TMPTA, we analyzed that the mass loss above 200 °C, and below 400 °C was the gradual evaporation of residual NVP, the mass loss at 400−450 °C was the gradual evaporation of TMPTA, and the mass loss at 450−600 was due to the gradual evaporation of PI. These mass losses are also consistent with our increase in the amount of each component.

2.7. Postcuring. The rapid molding of additive manufacturing makes the parts of photocuring a defect with a low

https://doi.org/10.1021/acsomega.1c06933
ACS Omega 2022, 7, 9582−9593

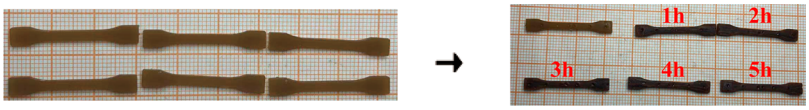

Figure 11. Shrinkage diagrams of the sample before and after heat curing at 190 °C for 0−5 h.

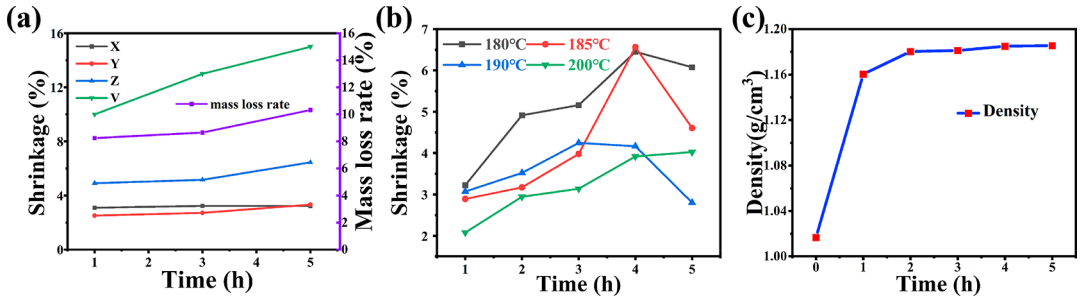

Figure 12. Change of thermal shrinkage rate: (a) shrinkage rate in *x*-, *y*-, and *z*-directions and volume shrinkage rate; (b) changes of shrinkage in the *z*-direction at different temperatures; (c) density change of prepared polyimide sample after heat curing for 1−5 h.

degree of cure. The work is enhanced by reinforcing the degree of cure after printing samples in the 190 °C blast drying tank, to expect its improvement integrated performance goals. System experiments show that thermal cure increases its degree of cure, which has great improvements to its hardness, shear modulus, and compression modulus.

2.8. Shrinkage Rate. The thermal curing increases its overall mechanical properties, which affects its dimensional stability. A large challenge facing light-curing polyimide is that the dimensional stability is poor, and the shrinkage is as high as 30−40%. However, fewer researchers have explored the system of contracting laws in their various directions, but the polyimide is considered to be associated with isotropic contractions. The group adopts the introduction of fluorine dihydride, chemical grafting techniques, and ester concentration, and the solution is greatly increased to increase its solubility in organic solvents; excellent solubility properties make it have a large solid content in an organic solvent. Thus, the resin obtained by this work exhibits smaller volume contraction after thermal curing (less than 20%; as shown in Figure 11). In addition, this work also systematically explores the contraction law of the photocurable polyimide resin in each direction and has made great contributions to the size stability in the polyimide.

System experiments show that the contraction in the planned direction of the print layer is consistent (as shown in Figure 12a, *x* and *y* directions), at 180 °C in 3−4%, while the contraction is perpendicular to the print layer plane (as shown in Figure 12a, *z* direction) and should be significantly higher than the contraction on the print layer plane; 180 °C remains around 8−10%. This is mainly due to the manufacture of a layer-by-layer stacked rapid molding, which is not sufficiently cured in the layer stack direction, and from the above discussion, thermal curing can significantly increase its degree of solidification, resulting in its mechanical properties being significantly increased, so different temperature thermal curing is still selected to explore its directional contraction changes. The results show that as the curing heat curing time is removed, the shrinkage in the *z* direction is gradually increased and shrunken in the *x* and *y* directions. When the shrinkage rate is maximized in 4 h, the shrinkage becomes small in 5 h because the polymer in hot curing is destroyed, causing cracking and thus the sample becoming smaller (as shown in Figure 12b). This is because the thermosetting layers are tighter in the gap between layers, and thus shrinkage gradually increases. In addition shrinkage in the *z* direction has no significant relationship with thermoset temperature, because the occurrence of imidation occurs.

3. CONCLUSIONS

In conclusion, on the basis of Kapton polyimide monomers PMDA and ODA with the best performance up to now, fluorine-containing diamine was introduced to change the structure of polyimide to make it easier to dissolve in the organic solvent, glycidyl methacrylate was introduced into its chain by chemical grafting technology, and finally, oligomer polyimide was obtained by maleic anhydride end-capping. Glycidyl methacrylate has two functions: on the one hand, it can introduce photocurable double bonds; on the other hand, it can enhance the adhesion between layers after resin curing to promote printing. In addition, in this work, the solubility of the prepared oligomer polyimide in organic solvent was greatly enhanced through three-step treatment, so that the oligomer polyimide dissolved in the organic solvent NVP had higher solubility, thus achieving higher solid content of printing resin to reduce its shrinkage. Then, the gradient porosity block structure with controllable shape is printed by digital light processing (DLP) equipment. The effects of different solid content, curing time, and single-layer printing thickness on its mechanical properties were deeply investigated. The shear strength and compressive strength of prepared polyimide are positively correlated with different solid content and curing time and negatively correlated with single-layer printing thickness. In this work, due to the modification of solubility and viscosity by grafting technology, the solid content can reach 40%. Moreover, this work explores for the first time the influence of the curing degree of thermal curing on its mechanical properties and finds out the best parameters (heating at 190 °C for 3−4 h) of thermal curing. Interestingly, in the process of exploring the influence of curing degree in this work, a novel phenomenon was found—the printing direction had a great influence on its shear strength. Given this, this work has made a systematic inquiry and made a reasonable explanation for this phenomenon for the first time. This phenomenon is mainly attributed to the molding method of photocuring layer-by-layer stacking manufacturing. In the layer

https://doi.org/10.1021/acsomega.1c06933
ACS Omega 2022, 7, 9582−9593

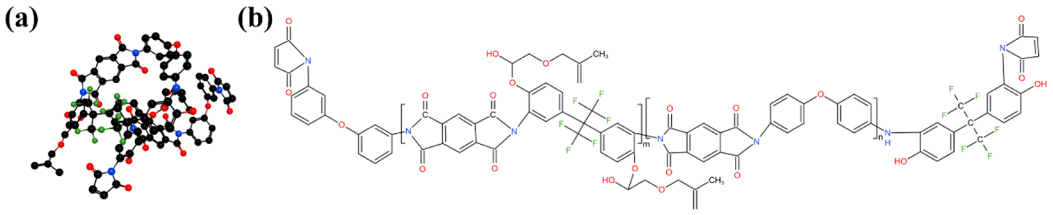

Figure 13. (a) Geometric configuration of preparation of oligomer polyimide. (b) Chemical formula of a structural unit of the final product for preparing polyimide oligomer.

stacking direction, because the bonding strength between layers is not as high as that in the horizontal direction, the mechanical properties in the vertical and horizontal printing layers are better than those in the horizontal printing layer direction. This phenomenon gradually weakens with the thermal curing, which is because the thermal curing makes the bonding between layers closer, so the performances gap between the two directions is obviously reduced. It is worth mentioning that the thermal stability of polyimide has always been its greatest advantage, and its long-term usable temperature can be between −200 and 300 °C, while the usable temperature of commercial resin that can be used for photocuring in the market is below 200 °C. Although the thermal decomposition temperature of the polyimide resin synthesized in this work is different from that of the traditional polyimide, it is still significantly better than the current photocuring resin. Therefore, this work is of great significance to areas with high demand for thermal stability, such as cooling valves, and has great reference value for the development and application of photocurable resin materials.

4. EXPERIMENTAL SECTION

4.1. Reagents and Materials. The main materials used in the experiment are as follows: hexafluoropropylene (6FOHA), 4,4′-diphenyl ether diamine (ODA), and homothallic acid dianhydride (PMDA), from Chem Pure, Shanghai Maclin Biochemical Technology Co., Ltd.; *N*-methylpyrrolidone (NMP), hydroquinone, triethylamine, tetraethylammonium bromide, maleic anhydride (MA), glycidyl methacrylate (GMA), *N*-vinylpyrrolidone (NVP), trimethylolpropane triacrylate (TMPTA), lauryl methacrylate (LMA), polyethylene glycol diacrylate (PEG400DA), from Chemical Pure, Shanghai Aladdin Biochemical Technology Co., Ltd.; (2,4,6-trimethylbenzoyl)diphenylphosphine oxide (TPO), Shanghai Bangcheng Chemical Co., Ltd.; and nitrogen.

4.2. Synthesis of Oligomer Polyimide. First, dianhydride and diamine monomers were dissolved in the organic polar solvent *N*-methylpyrrolidone under a nitrogen atmosphere at 0 °C. This was stirred evenly for 4 h until completely dissolved. Maleic anhydride was added as a capping agent and the mixture stirred for another 1 h. Then the temperature was gradually raised to 60, 110, and 205 °C for 2 h at constant temperature, respectively. The sample was cooled to room temperature; hydroquinone, triethylamine, tetraethylamine bromide, and glycidyl methacrylate (GMA) were added; and this was stirred well and then heated to 100 °C and stirred for 4 h until the reaction was complete. In the above steps, the brown liquid was stirred and poured into distilled water. After filtration and vacuum drying for 8 h, the light yellow polyimide oligomer powder was obtained (the resulting monomer is shown in Figure 13). The specific experimental process is shown in the summary chart. In addition, Figure 1 shows the reaction equation of the whole reaction process.

4.3. Preparation of Polyimide Resin. The oligomer polyimide powder was uniformly mixed with trimethylolpropane triacrylate (TMPTA), *N*-vinylpyrrolidone (NVP), and poly(ethylene glycol) 400 (PEGDA400) in a certain proportion. Then the photoinitiator with a 3% mass fraction was added and placed at 40 °C for constant temperature magnetic stirring for 4 h. Finally, the bubbles are removed in the centrifuge to obtain a polyimide resin which can be used as a photocurable additive.

4.4. Digital Light Processing Printing Polyimide Resin. The obtained polyimide resin was photocured and printed using a digital photoprocessing printer from Salomon. The polyimide resin was exposed and printed by an ultraviolet integrated lamp bead with a wavelength of 405 nm. The single-layer exposure time was 10−15 s, and the 3D object with a single-layer thickness of 10−50 μm could be generated.

4.5. Postprocessing. The DLP printed samples were placed in a constant-temperature blast drying oven for several hours to observe and test the shrinkage in all directions and the variation of mechanical properties with the oven temperature and time.

■ ASSOCIATED CONTENT

Supporting Information

The Supporting Information is available free of charge at https://pubs.acs.org/doi/10.1021/acsomega.1c06933.

Structure characterization through NMR spectroscopy, sample sizes of tensile shear and compression tests included in this work for reference (Figures S1 and S2) (PDF)

■ AUTHOR INFORMATION

Corresponding Author

Guoqiang Luo − *Chaozhou Branch of Chemistry and Chemical Engineering Guangdong Laboratory, Chaozhou 521000, China; State Key Laboratory of Advanced Technology for Materials Synthesis and Processing, Wuhan University of Technology, Wuhan 430070, China;* orcid.org/0000-0001-7879-0012; Email: luogq@whut.edu.cn

Authors

Zhiqiang Liu − *State Key Laboratory of Advanced Technology for Materials Synthesis and Processing, Wuhan University of Technology, Wuhan 430070, China*

Yilun Cai − *Hospital of Wuhan University of Technology, Wuhan University of Technology, Wuhan 430070, China*

Feifan Song − *State Key Laboratory of Advanced Technology for Materials Synthesis and Processing, Wuhan University of Technology, Wuhan 430070, China*

https://doi.org/10.1021/acsomega.1c06933
ACS Omega 2022, 7, 9582−9593

Jiajin Li − *State Key Laboratory of Advanced Technology for Materials Synthesis and Processing, Wuhan University of Technology, Wuhan 430070, China*
Jian Zhang − *State Key Laboratory of Advanced Technology for Materials Synthesis and Processing, Wuhan University of Technology, Wuhan 430070, China*
Yi Sun − *State Key Laboratory of Advanced Technology for Materials Synthesis and Processing, Wuhan University of Technology, Wuhan 430070, China*
Qiang Shen − *State Key Laboratory of Advanced Technology for Materials Synthesis and Processing, Wuhan University of Technology, Wuhan 430070, China*

Complete contact information is available at: https://pubs.acs.org/10.1021/acsomega.1c06933

Author Contributions

Z.L.: Investigation, methodology, writing—original draft, formal analysis, and data curation. Y.C.: Methodology, resources, and writing—review and editing. F.S.: Methodology and formal analysis. J.L.: Methodology and formal analysis. J.Z.: Methodology, resources, writing—review and editing, and data curation. Y.S.: Methodology, resources, writing—review and editing, and data curation. G.L.: Methodology, resources, project administration, writing—review and editing, and data curation. Q.S.: Methodology, resources, and project administration.

Author Contributions

[‖]Z.L. and Y.C. contributed equally to this work.

Notes

The authors declare no competing financial interest.

■ ACKNOWLEDGMENTS

We are grateful for the financial support received from the National Key R&D Program of China (Grant No. 2021YFB3802300), Guangdong Major Project of Basic and Applied Basic Research (Grant No. 2021B0301030001), Key-Area Research and Development Program of Guangdong Province (Grant No. 2020B010181001), National Natural Science Foundation (Grant No. 51932006), and Basic Strengthening Project of Science and Technology Commission of CMC (Grant No. 202022JQ01).

■ REFERENCES

(1) Chen, L.; Wu, Q.; Wei, G.; Liu, R.; Li, Z. Highly stable thiol−ene systems: from their structure−property relationship to DLP 3D printing. *J. Mater. Chem. C* **2018**, *6*, 11561−11568.
(2) Marino, A.; Barsotti, J.; de Vito, G.; Filippeschi, C.; Mazzolai, B.; Piazza, V.; Labardi, M.; Mattoli, V.; Ciofani, G. Two-Photon Lithography of 3D Nanocomposite Piezoelectric Scaffolds for Cell Stimulation. *ACS Appl. Mater. Interfaces* **2015**, *7*, 25574−9.
(3) Zhang, H.; Moon, S. K. Reviews on Machine Learning Approaches for Process Optimization in Noncontact Direct Ink Writing. *ACS Appl. Mater. Interfaces* **2021**, *13*, 53323−53345.
(4) Liu, L.; Liu, S.; Schelp, M.; Chen, X. Rapid 3D Printing of Bioinspired Hybrid Structures for High-Efficiency Fog Collection and Water Transportation. *ACS Appl. Mater. Interfaces* **2021**, *13*, 29122−29129.
(5) Bain, E. D., Polymer Powder Bed Fusion Additive Manufacturing: Recent Developments in Materials, Processes, and Applications. In *Polymer-Based Additive Manufacturing: Recent Developments*; American Chemical Society, 2019; Vol. *1315*, pp 7−36. DOI: 10.1021/bk-2019-1315.ch002.
(6) Ligon, S. C.; Liska, R.; Stampfl, J.; Gurr, M.; Mulhaupt, R. Polymers for 3D Printing and Customized Additive Manufacturing. *Chem. Rev.* **2017**, *117*, 10212−10290.
(7) Bagheri, A.; Jin, J. *Photopolymerization in 3D Printing* **2019**, *1* (4), 593−611.
(8) Zhou, Z. X.; Li, Y.; Zhong, J.; Luo, Z.; Gong, C. R.; Zheng, Y. Q.; Peng, S.; Yu, L. M.; Wu, L.; Xu, Y. High-Performance Cyanate Ester Resins with Interpenetration Networks for 3D Printing. *ACS Appl. Mater. Interfaces* **2020**, *12*, 38682−38689.
(9) Dizon, J. R. C.; Espera, A. H.; Chen, Q.; Advincula, R. C. Mechanical characterization of 3D-printed polymers. *Addit. Manuf.* **2018**, *20*, 44−67.
(10) Ji, Z.; Jiang, D.; Zhang, X.; Guo, Y.; Wang, X. Facile Photo and Thermal Two-Stage Curing for High-Performance 3D Printing of Poly(Dimethylsiloxane). *Macromol. Rapid Commun.* **2020**, *41*, 2000064.
(11) Heidenreich, A. C.; Pérez-Recalde, M.; González Wusener, A.; Hermida, É. B. Collagen and chitosan blends for 3D bioprinting: A rheological and printability approach. *Polym. Test.* **2020**, *82*, 106297.
(12) Shen, Y.; Tang, H.; Huang, X.; Hang, R.; Zhang, X.; Wang, Y.; Yao, X. DLP printing photocurable chitosan to build bio-constructs for tissue engineering. *Carbohydr. Polym.* **2020**, *235*, 115970.
(13) Peng, X.; Kuang, X.; Roach, D. J.; Wang, Y.; Hamel, C. M.; Lu, C.; Qi, H. J. Integrating digital light processing with direct ink writing for hybrid 3D printing of functional structures and devices. *Addit. Manuf.* **2021**, *40*, 101911.
(14) Mirzaali, M. J.; Cruz Saldívar, M.; Herranz de la Nava, A.; Gunashekar, D.; Nouri-Goushki, M.; Doubrovski, E. L.; Zadpoor, A. A. Multi-Material 3D Printing of Functionally Graded Hierarchical Soft−Hard Composites. *Adv. Eng. Mater.* **2020**, *22*, 1901142.
(15) Gu, W.; Wang, G.; Zhou, M.; Zhang, T.; Ji, G. Polyimide-Based Foams: Fabrication and Multifunctional Applications. *ACS Appl. Mater. Interfaces* **2020**, *12*, 48246−48258.
(16) Heng, H.; Yang, J.; Yin, Y.; Meng, P.; Liu, X. Effect of precursor types on the performance of polyimide: A metal-free visible-light-driven photocatalyst for effective photocatalytic degradation of pollutants. *Catal. Today* **2020**, *340*, 225−235.
(17) Song, Z.; Zhan, H.; Zhou, Y. Polyimides: promising energy-storage materials. *Angew. Chem., Int. Ed. Engl.* **2010**, *49*, 8444−8.
(18) Liaw, D.-J.; Wang, K.-L.; Huang, Y.-C.; Lee, K.-R.; Lai, J.-Y.; Ha, C.-S. Advanced polyimide materials: Syntheses, physical properties and applications. *Prog. Polym. Sci.* **2012**, *37*, 907−974.
(19) Gouzman, I.; Grossman, E.; Verker, R.; Atar, N.; Bolker, A.; Eliaz, N. Advances in Polyimide-Based Materials for Space Applications. *Adv. Mater.* **2019**, *31*, 1807738.
(20) Hegde, M.; Meenakshisundaram, V.; Chartrain, N.; Sekhar, S.; Tafti, D.; Williams, C. B.; Long, T. E. 3D Printing All-Aromatic Polyimides using Mask-Projection Stereolithography: Processing the Nonprocessable. *Adv. Mater.* **2017**, *29* (31), 1701240.
(21) Herzberger, J.; Meenakshisundaram, V.; Williams, C. B.; Long, T. E. 3D Printing All-Aromatic Polyimides Using Stereolithographic 3D Printing of Polyamic Acid Salts. *ACS Macro Lett.* **2018**, *7*, 493−497.
(22) Rau, D. A.; Herzberger, J.; Long, T. E.; Williams, C. B. Ultraviolet-Assisted Direct Ink Write to Additively Manufacture All-Aromatic Polyimides. *ACS Appl. Mater. Interfaces* **2018**, *10* (41), 34828−34833.
(23) Mohamed, M. G.; Kuo, S. W. Functional Polyimide/Polyhedral Oligomeric Silsesquioxane Nanocomposites. *Polymers (Basel)* **2019**, *11* (1), 26.
(24) Rusu, R.-D.; Constantin, C.-P.; Drobota, M.; Gradinaru, L.-M.; Butnaru, M.; Pislaru, M. Polyimide films tailored by UV irradiation: Surface evaluation and structure-properties relationship. *Polym. Degrad. Stab.* **2020**, *177*, 109182.
(25) Shi, G.; Kim, J.; Baek, K.; Bae, J.; Park, L. S. Melt and One-Pot Solution Synthesis of Thermally Stable, Organosoluble and Photocurable Acidic Polyimides. *Materials Sciences and Applications* **2019**, *10*, 709−720.

(26) Guo, Y.; Ji, Z.; Zhang, Y.; Wang, X.; Zhou, F. Solvent-free and photocurable polyimide inks for 3D printing. *J. Mater. Chem. A* **2017**, *5*, 16307−16314.
(27) Guo, Y.; Xu, J.; Yan, C.; Chen, Y.; Zhang, X.; Jia, X.; Liu, Y.; Wang, X.; Zhou, F. Direct Ink Writing of High Performance Architectured Polyimides with Low Dimensional Shrinkage. *Adv. Eng. Mater.* **2019**, *21* (5), 1801314.
(28) Li, X.; Yang, Y.; Zhang, Y.; Wang, T.; Yang, Z.; Wang, Q.; Zhang, X. Dual-method molding of 4D shape memory polyimide ink. *Mater. Des.* **2020**, *191*, 108606.
(29) Arrington, C. B.; Rau, D. A.; Williams, C. B.; Long, T. E. UV-assisted direct ink write printing of fully aromatic Poly(amide imide)s: Elucidating the influence of an acrylic scaffold. *Polymer* **2021**, *212*, 123306.
(30) Wu, T.; Jiang, P.; Zhang, X.; Guo, Y.; Ji, Z.; Jia, X.; Wang, X.; Zhou, F.; Liu, W. Additively manufacturing high-performance bismaleimide architectures with ultraviolet-assisted direct ink writing. *Mater. Des.* **2019**, *180*, 107947.
(31) Wang, C.; Ma, S.; Li, D.; Zhao, J.; Zhou, H.; Wang, D.; Zhou, D.; Gan, T.; Wang, D.; Liu, C.; Qu, C.; Chen, C. 3D Printing of Lightweight Polyimide Honeycombs with the High Specific Strength and Temperature Resistance. *ACS Appl. Mater. Interfaces* **2021**, *13*, 15690−15700.
(32) Ji, Z.; Zhang, X.; Yan, C.; Jia, X.; Xia, Y.; Wang, X.; Zhou, F. 3D Printing of Photocuring Elastomers with Excellent Mechanical Strength and Resilience. *Macromol. Rapid Commun.* **2019**, *40*, 1800873.
(33) Zhou, J.; Allonas, X.; Ibrahim, A.; Liu, X. Progress in the development of polymeric and multifunctional photoinitiators. *Prog. Polym. Sci.* **2019**, *99*, 101165.
(34) Huang, Y.; Leu, M. C.; Mazumder, J.; Donmez, A. Additive Manufacturing: Current State, Future Potential, Gaps and Needs, and Recommendations. *J. Manuf. Sci. Eng.* **2015**, *137* (1), 014001.
(35) Wu, W.; Ye, W.; Geng, P.; Wang, Y.; Li, G.; Hu, X.; Zhao, J. 3D printing of thermoplastic PI and interlayer bonding evaluation. *Mater. Lett.* **2018**, *229*, 206−209.
(36) del Barrio, J.; Sánchez-Somolinos, C. Light to Shape the Future: From Photolithography to 4D Printing. *Adv. Opt. Mater.* **2019**, *7* (16), 1900598.
(37) Améduri, B. The Promising Future of Fluoropolymers. *Macromol. Chem. Phys.* **2020**, *221*, 1900573.
(38) Zhang, M.; Liu, W.; Gao, X.; Cui, P.; Zou, T.; Hu, G.; Tao, L.; Zhai, L. Preparation and Characterization of Semi-alicyclic Polyimides Containing Trifluoromethyl Groups for Optoelectronic Application. *Polymers (Basel)* **2020**, *12* (7), 1532.
(39) Yi, L.; Huang, W.; Yan, D. Polyimides with side groups: Synthesis and effects of side groups on their properties. *J. Polym. Sci., Part A: Polym. Chem.* **2017**, *55*, 533−559.
(40) Cao, S.; Chen, Q.; Wang, Y.; Xuan, S.; Jiang, W.; Gong, X. High strain-rate dynamic mechanical properties of Kevlar fabrics impregnated with shear thickening fluid. *Composites, Part A* **2017**, *100*, 161−169.
(41) Voet, V. S. D.; Strating, T.; Schnelting, G. H. M.; Dijkstra, P.; Tietema, M.; Xu, J.; Woortman, A. J. J.; Loos, K.; Jager, J.; Folkersma, R. Biobased Acrylate Photocurable Resin Formulation for Stereolithography 3D Printing. *ACS Omega* **2018**, *3*, 1403−1408.
(42) Zhang, F.; Tuck, C.; Hague, R.; He, Y.; Saleh, E.; Li, Y.; Sturgess, C.; Wildman, R. Inkjet printing of polyimide insulators for the 3D printing of dielectric materials for microelectronic applications. *J. Appl. Polym. Sci.* **2016**, *133*, 43361.
(43) Kuang, X.; Zhao, Z.; Chen, K.; Fang, D.; Kang, G.; Qi, H. J. High-Speed 3D Printing of High-Performance Thermosetting Polymers via Two-Stage Curing. *Macromol. Rapid Commun.* **2018**, *39*, 1700809.
(44) Weigand, J. J.; Miller, C. I.; Janisse, A. P.; McNair, O. D.; Kim, K.; Wiggins, J. S. 3D printing of dual-cure benzoxazine networks. *Polymer* **2020**, *189*, 122193.
(45) Albrecht Ludwig Harreus, R.; Backes, J.-O.; Eichler, R.; Feuerhake, C.; Jäkel, U.; Mahn, R.; Pinkos, R. 2-Pyrrolidone. *Ullmann's Encyclopedia of Industrial Chemistry*, 7th ed.; Wiley-VCH: Weinheim, Germany, 2011.
(46) Guerra, A.; Koch, L.; Lindberg, S. The Dirichlet problem for the Jacobian equation in critical and supercritical Sobolev spaces. *Calculus Var. Partial Differ. Equations* **2021**, *60*, 55.
(47) Pan, Y.; He, H.; Xu, J.; Feinerman, A. Study of separation force in constrained surface projection stereolithography. *Rapid Prototyping J.* **2017**, *23*, 353−361.
(48) Hayki, N.; Lecamp, L.; Désilles, N.; Lebaudy, P. Kinetic Study of Photoinitiated Frontal Polymerization. Influence of UV Light Intensity Variations on the Conversion Profiles. *Macromolecules* **2010**, *43*, 177−184.
(49) Huang, Y.-M.; Jiang, C.-P. On-line force monitoring of platform ascending rapid prototyping system. *J. Mater. Process. Technol.* **2005**, *159*, 257−264.
(50) Gofman, I.; Nikolaeva, A.; Yakimansky, A.; Ivanova, O.; Baranchikov, A.; Ivanov, V. Unexpected selective enhancement of the thermal stability of aromatic polyimide materials by cerium dioxide nanoparticles. *Polym. Adv. Technol.* **2019**, *30*, 1518−1524.
(51) Çakir, M.; Kılıç, V.; Boztoprak, Y.; Özmen, F. K. Graphene oxide-containing isocyanate-based polyimide foams: Enhanced thermal stability and flame retardancy. *J. Appl. Polym. Sci.* **2021**, *138*, 51012.
(52) Cuesta, E.; Alvarez, B. J.; Zapico, P.; Giganto, S. Analysis of post-processing influence on the geometrical and dimensional accuracy of selective laser melting parts. *Rapid Prototyping J.* **2020**, *26*, 1713−1722.
(53) Jindal, P.; Juneja, M.; Bajaj, D.; Siena, F. L.; Breedon, P. Effects of post-curing conditions on mechanical properties of 3D printed clear dental aligners. *Rapid Prototyping J.* **2020**, *26*, 1337−1344.
(54) Kim, D. S. D.; Suriboot, J.; Shih, C.-C.; Cwiklik, A.; Grunlan, M. A.; Tai, B. L. Mechanical isotropy and postcure shrinkage of polydimethylsiloxane printed with digital light processing. *Rapid Prototyping J.* **2020**, *26*, 1447−1452.

https://doi.org/10.1021/acsomega.1c06933
ACS Omega 2022, 7, 9582−9593